

Short-Wavelength Flash Photolytic Fragmentation of $\text{Ru}_3(\text{CO})_{12}$ in the Presence of CO and Complementary Experiments with $\text{Ru}(\text{CO})_5$: A Time-Resolved IR Spectroscopic Study

Friedrich-Wilhelm Grevels,* Werner E. Klotzbücher, Jörg Schrickel, and Kurt Schaffner

Contribution from the Max-Planck-Institut für Strahlenchemie, Stiftstrasse 34-36, Postfach 10 13 65, D-45413 Mülheim an der Ruhr, Federal Republic of Germany

Received November 15, 1993. Revised Manuscript Received April 12, 1994*

Abstract: Short-wavelength (308 nm) photoinduced reactions of binary ruthenium carbonyls in the presence of varying concentrations of carbon monoxide are investigated by means of flash photolysis (XeCl excimer laser) in combination with time-resolved IR spectroscopy. Photodissociation of CO from $\text{Ru}_3(\text{CO})_{12}$ yields the $\text{Ru}_3(\text{CO})_{11}$ fragment in the CO-bridged form. Beyond the known re-formation of the parent complex, this species under CO atmosphere takes up a total number of three CO ligands to form a 1:1 mixture of $\text{Ru}(\text{CO})_5$ and $\text{Ru}_2(\text{CO})_9$, as the ultimately observed products. This process involves the intermediate formation of $\text{Ru}_3(\text{CO})_{12}(\mu\text{-CO})$, which decays by first-order kinetics with a rate constant of about $2.2 \times 10^4 \text{ s}^{-1}$ at ambient temperature. Complementary studies with $\text{Ru}(\text{CO})_5$ and (*in situ* generated) $\text{Ru}_2(\text{CO})_9$ as starting materials provide insight into the mechanism by which $\text{Ru}(\text{CO})_5$ is converted into $\text{Ru}_3(\text{CO})_{12}$ and/or $\text{Ru}_2(\text{CO})_9$, depending on the CO concentration and the photolysis conditions. The solvated $\text{Ru}(\text{CO})_4$ fragment, the dinuclear $\text{Ru}_2(\text{CO})_8$, and $\text{Ru}_3(\text{CO})_{12}(\mu\text{-CO})$ are observed as transient species in addition to $\text{Ru}_2(\text{CO})_9$, which is stable on the time scale of these experiments.

Introduction

The photolytic behavior of $\text{Ru}_3(\text{CO})_{12}$ (1) in the presence of carbon monoxide or other potential ligands L depends on the wavelength of irradiation, the nature of L, the solvent, and the temperature.¹ In essence, two different types of processes are observed, *viz.*, cluster cleavage and CO substitution.

Breakdown of the trinuclear cluster with formation of mononuclear products reportedly occurs from the lowest-energy excited state of $\text{Ru}_3(\text{CO})_{12}$, which is populated upon irradiation into the characteristic long-wavelength absorption band, centered around 392 nm, and is thought to be antibonding with respect to the Ru_3 core framework.² This process proved to be very useful for the conversion of $\text{Ru}_3(\text{CO})_{12}$ into $\text{Ru}(\text{CO})_5$ and its *n*-donor- or olefin-substituted derivatives,^{3–9} the latter being particularly relevant

to various photocatalytic processes.⁸ A CO-bridged isomeric species (1-B) of $\text{Ru}_3(\text{CO})_{12}$ has been invoked^{6,9} as the primary photoproduct, which offers a vacant coordination site to the incoming ligand L and thus could form the $\text{Ru}_3(\text{CO})_{12}\text{L}$ adduct (2, 3) as a key intermediate (Scheme 1). Further addition of L with concomitant metal–metal bond fission ultimately yields three mononuclear product molecules (6, 7), probably via the intermediate formation of the dinuclear species $\text{Ru}_2(\text{CO})_8\text{L}$ (4, 5). As an alternative process, loss of CO from 2 would provide a rationale for the associative photosubstitution of CO observed at lower temperatures to yield $\text{Ru}_3(\text{CO})_{11}\text{L}$ (8).¹⁰

Dissociative CO photosubstitution^{9,11} occurs upon irradiation of $\text{Ru}_3(\text{CO})_{12}$ at shorter wavelengths (Scheme 2). IR spectroscopic studies in low-temperature glasses revealed the existence of two isomeric forms of the primary photofragment $\text{Ru}_3(\text{CO})_{11}$ (9), one with only terminal CO ligands (9-T) and the other (9-B) with at least one bridging CO group.¹⁰ The latter apparently is more stable and also has been observed as a short-lived transient by means of time-resolved IR spectroscopy, following its generation by laser flash photolysis ($\lambda = 308 \text{ nm}$) of $\text{Ru}_3(\text{CO})_{12}$ in hydrocarbon solution at ambient temperature.¹¹ In the presence of low to moderate concentrations of added CO (under 99:1 to 90:10 Ar–CO atmosphere), the decay of the transient absorptions of 9-B follows pseudo-first-order kinetics with re-formation of $\text{Ru}_3(\text{CO})_{12}$ (1) as the only observed process.¹¹

We wish to report on the unexpected finding that under analogous short-wavelength photolysis conditions, but in the presence of CO in higher concentration (e.g., under neat CO atmosphere), the reversibility of the system is lost. This investigation not only allows us to establish a link between photodissociation of CO from $\text{Ru}_3(\text{CO})_{12}$ (Scheme 2) and the breakdown of the trinuclear cluster framework (Scheme 1) but also provides the first IR spectroscopic evidence of the transient existence of the elusive $\text{Ru}_3(\text{CO})_{13}$ species (3). Additional

* Abstract published in *Advance ACS Abstracts*, June 1, 1994.

(1) For a recent excellent review, see: Ford, P. C. *J. Organomet. Chem.* **1990**, *383*, 339–356.

(2) (a) Tyler, D. R.; Levenson, R. A.; Gray, H. B. *J. Am. Chem. Soc.* **1978**, *100*, 7888–7893. (b) Delley, B.; Manning, M. C.; Ellis, D. E.; Berkowitz, J.; Troglor, W. C. *Inorg. Chem.* **1982**, *21*, 2247–2253.

(3) (a) Johnson, B. F. G.; Lewis, J.; Twigg, M. V. *J. Organomet. Chem.* **1974**, *67*, C75–C76. (b) Johnson, B. F. G.; Lewis, J.; Twigg, M. V. *J. Chem. Soc., Dalton Trans.* **1975**, 1876–1879.

(4) Gregory, M. F.; Poliakoff, M.; Turner, J. J. *J. Mol. Struct.* **1985**, *127*, 247–256.

(5) (a) Grevels, F.-W.; Reuvers, J. G. A.; Takats, J. *J. Am. Chem. Soc.* **1981**, *103*, 4069–4073. (b) Ball, R. G.; Kiel, G.-Y.; Takats, J.; Krüger, C.; Raabe, E.; Grevels, F.-W.; Moser, R. *Organometallics* **1987**, *6*, 2260–2261.

(c) Grevels, F.-W.; Reuvers, J. G. A.; Takats, J. *Inorg. Synth.* **1986**, *24*, 176–180.

(6) (a) Malito, J.; Markiewicz, S.; Poë, A. *Inorg. Chem.* **1982**, *21*, 4335–4337. (b) Brodie, N. M. J.; Huq, R.; Malito, J.; Markiewicz, S.; Poë, A. J.; Sekhar, V. C. *J. Chem. Soc., Dalton Trans.* **1989**, 1933–1939.

(7) Alex, R. F.; Pomeroy, R. K. *Organometallics* **1982**, *1*, 453–459.

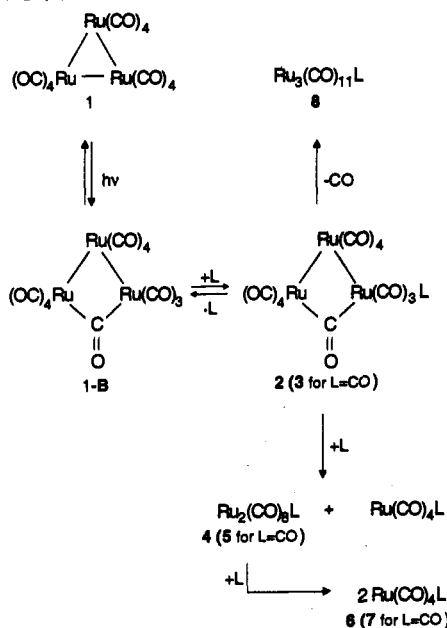
(8) (a) Austin, R.; Paonessa, R. S.; Giordano, P. J.; Wrighton, M. S. *Adv. Chem. Ser.* **1978**, *68*, 189–212. (b) Graff, J. L.; Sanner, R. D.; Wrighton, M. S. *J. Am. Chem. Soc.* **1979**, *101*, 273–275. (c) Graff, J. L.; Sanner, R. D.; Wrighton, M. S. *Organometallics* **1982**, *1*, 837–842. (d) Wu, Y.-M.; Bentsen, J. G.; Brinkley, C. G.; Wrighton, M. S. *Inorg. Chem.* **1987**, *26*, 530–540.

(9) (a) Desrosiers, M. F.; Ford, P. C. *Organometallics* **1982**, *1*, 1715–1716. (b) Desrosiers, M. F.; Wink, D. A.; Ford, P. C. *Inorg. Chem.* **1985**, *24*, 1–2. (c) Desrosiers, M. F.; Wink, D. A.; Trautman, R.; Friedman, A. E.; Ford, P. C. *J. Am. Chem. Soc.* **1986**, *108*, 1917–1927.

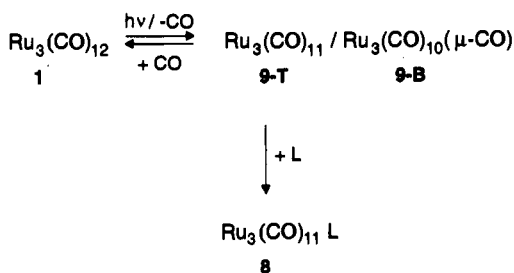
(10) Bentsen, J. G.; Wrighton, M. S. *J. Am. Chem. Soc.* **1987**, *109*, 4530–4544.

(11) DiBenedetto, J. A.; Ryba, D. W.; Ford, P. C. *Inorg. Chem.* **1989**, *28*, 3503–3507.

Scheme 1. Proposed Mechanism of the Long-Wavelength Photoinduced Fragmentation and Associative Substitution of $\text{Ru}_3(\text{CO})_{12}$ (1)



Scheme 2. Short-Wavelength Photoinduced Dissociative Substitution of $\text{Ru}_3(\text{CO})_{12}$ (1)



information is obtained from complementary experiments using $\text{Ru}(\text{CO})_5$ as the starting material.

Experimental Section

$\text{Ru}_3(\text{CO})_{12}$ was purchased from Strem Chemicals and used as received. Dilute solutions (ca. 1 mM) of $\text{Ru}(\text{CO})_5$ were prepared by continuous irradiation of $\text{Ru}_3(\text{CO})_{12}$ in CO-saturated 2-methylpentane or methylcyclohexane at ambient temperature,^{3a} using a high-pressure mercury lamp (Philips HPK, 125 W) and an immersion well irradiation apparatus¹² equipped with a GWV (Glaswerk Wertheim) cutoff filter tube ($\lambda \geq 370$ nm); dissolved CO was removed by several freeze-pump-thaw cycles, unless otherwise noted. Cyclohexane (Merck, analytical grade), methylcyclohexane, and 2-methylpentane (Merck, synthetic grade) were purified by distillation and checked for residual trace impurities by means of gas chromatography and UV-vis spectroscopy. High-purity argon (6.0) and carbon monoxide (4.7) gases were purchased from Messer-Griesheim.

The instrumentation for flash photolysis with time-resolved IR detection has been described elsewhere.¹³ The actual configuration used in the present studies, involving the Lambda Physik EMG 200 excimer laser ($\lambda = 308$ nm with XeCl; output attenuated to 80–90 mJ/pulse) as the excitation light source and the globar as the monitoring IR light source, has a system response time of 1–2 μs and a spectral resolution of 3–4 cm^{-1} . Flash photolysis experiments with $\text{Ru}_3(\text{CO})_{12}$ were performed at ambient temperature, whereas for the experiments with $\text{Ru}(\text{CO})_5$, the reservoir and the IR sample cell were modified for cooling to -20 °C and 5 ± 2 °C, respectively. The routine procedure for preparing the stock solution involves at least three freeze-pump-thaw cycles, followed by

(12) Grevels, F.-W.; Reuvers, J. G. A.; Takats, J. *Inorg. Synth.* 1986, 24, 176–180.

(13) Schaffner, K.; Grevels, F.-W. *J. Mol. Struct.* 1988, 173, 51–65.

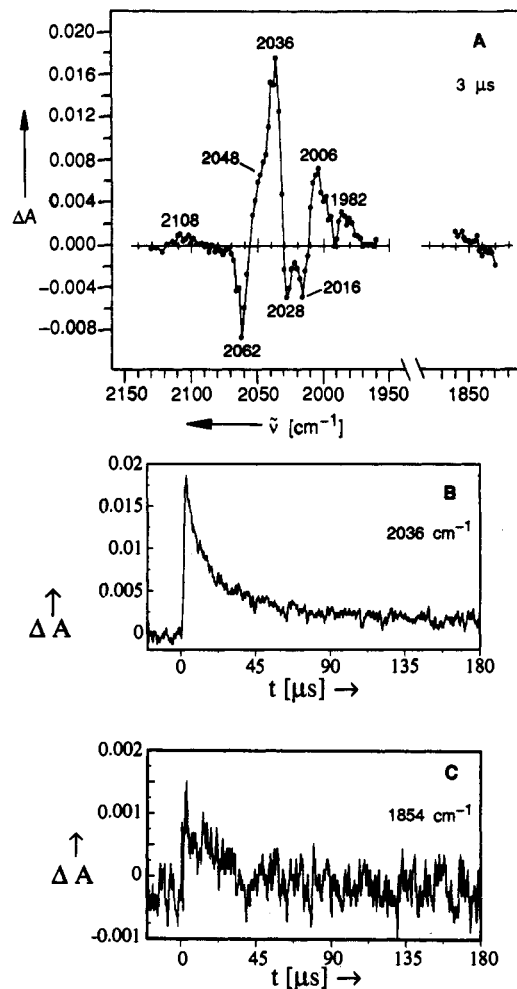


Figure 1. (A) Transient CO stretching vibrational IR difference spectrum recorded 3 μs after 308-nm flash photolysis of $\text{Ru}_3(\text{CO})_{12}$ (1, 0.6 mM) in cyclohexane under Ar atmosphere at ambient temperature. (B) and (C) Decay of the photogenerated $\text{Ru}_3(\text{CO})_{10}(\mu\text{-CO})$ fragment (9-B) monitored at 2036 and 1854 cm^{-1} ; note the difference in the ΔA scales.

saturation with the desired gas atmosphere in the reservoir, which is pressurized to 1.5 bar. Unless otherwise noted, in the intervals between the individual laser shots, the cell was emptied and refilled with fresh stock solution from the reservoir through a magnetic valve system.

Continuous photolysis at -50 °C was performed in a variable-temperature IR cell (CaF_2 windows, mounted with indium gaskets; $d = 1$ mm), cooled with a stream of cold nitrogen gas, the outer jacket flushed with dry argon. A Hanovia 1000-W high pressure Xe/Hg lamp, in combination with a Schoeffel Instruments GM 252 grating monochromator and a fiber optic, was employed for monochromatic irradiation.

Results and Discussion

A. Flash Photolysis of $\text{Ru}_3(\text{CO})_{12}$. Time-resolved IR detection of the primary photoproduct generated from $\text{Ru}_3(\text{CO})_{12}$ upon laser flash photolysis (XeCl excimer laser, $\lambda = 308$ nm) in cyclohexane solution (0.6 mM) under argon atmosphere essentially confirms the previous observation by Ford and co-workers¹¹ of a short-lived species assignable as the CO-bridged isomer 9-B of the $\text{Ru}_3(\text{CO})_{11}$ fragment (Scheme 2). The transient IR difference spectrum displayed in Figure 1A covers the entire terminal ν_{CO} region from 2130 to 1960 cm^{-1} and thus complements the previously observed spectrum¹¹ in both directions, i.e., to higher and lower monitoring wavenumbers. The depletion band minima of $\text{Ru}_3(\text{CO})_{12}$ (1) at 2062, 2028, and 2016 cm^{-1} are slightly different from those in a conventional IR spectrum [2060.5 (vst), 2031 (st), 2017 (w), and 2011 (m) cm^{-1} ; Table 1], because of partial overlap with the positive product absorptions. The latter comprise a weak feature at 2108 cm^{-1} , a strong band at 2036

Table 1. CO Stretching Vibrations [cm^{-1}] in the IR Spectra of $\text{Ru}_3(\text{CO})_{12}$ (1) and Photogenerated Products

$\text{Ru}_3(\text{CO})_{12}$ (1) ^a	2060.5 (vst), 2031 (st), 2017 (w), 2011 (m)
$\text{Ru}_3(\text{CO})_{12}(\mu\text{-CO})$ (3) ^b	2090 (m), 2052 (vst), 1996 (w), 1980 (m), 1796 (w)
$\text{Ru}_2(\text{CO})_9$ (5) ^a	2078 (m), 2039.5 (vst), 2029 (w), 2018.5 (st), 2005.5 (vw), 1813 (m)
$\text{Ru}(\text{CO})_5$ (7) ^a	2038.5 (st), 2000 (vst)
$\text{Ru}_3(\text{CO})_{10}(\mu\text{-CO})$ (9-B) ^b	2108 (w), 2048 (sh), 2036 (vst), 2006 (m), 1982 (m), 1840–1860 (w)
$\text{Ru}(\text{CO})_4\text{-C}_6\text{D}_6$ (11) ^b	2096 (w), 1984 (st), 1958 (st)
$\text{Ru}_2(\text{CO})_8$ (12) ^b	2066 (see text)

^a From conventional FT-IR spectra. ^b From time-resolved IR difference spectra; band positions may be subject to small changes arising from varying overlap with depletion bands.

cm^{-1} (cf. Figure 1B) with a shoulder near 2048 cm^{-1} , and two absorptions of medium intensity at 2006 and 1982 cm^{-1} . This pattern compares well with the terminal ν_{CO} absorptions of the CO-bridged form of the $\text{Ru}_3(\text{CO})_{11}$ fragment (9-B), observed in a low-temperature methylcyclohexane glass [2107 (w), 2063 (st), 2039 (sh), 2033 (vst), 2023 (st), 2005 (m), 1975 (m), and 1935 (vw) cm^{-1}],^{10,14} and is also in accord with the previously reported time-resolved IR data [2036 (st) and 2047 (w) cm^{-1}]¹¹ of this species. Moreover, an albeit barely discernible, broad feature located around 1840–1860 cm^{-1} (cf. Figures 1A and 1C) in the bridging ν_{CO} region provides direct evidence of the bridging CO group, although this weak band is slightly shifted compared with its reported position in methylcyclohexane glass (1836 cm^{-1}).¹⁰

The fate of this photogenerated $\text{Ru}_3(\text{CO})_{10}(\mu\text{-CO})$ fragment (9-B)¹⁵ strongly depends on the concentration of carbon monoxide present in the solution. Under argon atmosphere, it decays within a period of 40–50 μs (Figures 1B and 1C) with concurrent reformation of $\text{Ru}_3(\text{CO})_{12}$. The system is not entirely reversible, but the residual absorptions are of only minor intensities. These observations are qualitatively in accord with the previous findings of Ford and co-workers¹¹ (Scheme 2), who reported that under argon atmosphere the positive transient absorption and depletion features decay by second-order kinetics with an estimated rate constant of $k = 5 \times 10^9 \text{ M}^{-1} \text{ s}^{-1}$. Moreover, these authors have demonstrated that this process is greatly accelerated in the presence of added carbon monoxide. Thus, under 90:10 Ar–CO atmosphere, a pseudo-first-order rate constant $k_{\text{obs}} = (2.2 \pm 0.4) \times 10^6 \text{ s}^{-1}$ has been measured.¹¹

We note that, at higher concentrations of added CO, the lifetime of the $\text{Ru}_3(\text{CO})_{10}(\mu\text{-CO})$ fragment (9-B) is further reduced and approaches (or even falls below) the limits of the response time of our instrumentation (1–2 μs). Under a 2:1 Ar–CO atmosphere, the transient existence of this species is just still recognizable, as indicated by the appearance of a narrow spike in the transient absorbance traces at monitoring wavenumbers around 2032–2042 (Figure 2D) and 2004–2008 cm^{-1} . The initially observed spectrum (Figure 2A) closely resembles the one recorded under argon atmosphere (Figure 1A), but obviously both the depletion bands and the positive absorptions are substantially reduced in intensity. Thus we conclude that a major proportion of the

(14) The $\text{Ru}_3(\text{CO})_{11}$ fragment absorptions at 2063 and 2023 cm^{-1} are not observed in the time-resolved IR difference spectrum due to the overlap with the parent $\text{Ru}_3(\text{CO})_{12}$ depletion bands, while the very weak band at 1935 cm^{-1} apparently is below the detection limit.

(15) Our IR data do not allow us to draw unambiguous conclusions concerning the structure of the CO-bridged $\text{Ru}_3(\text{CO})_{11}$ fragment 9-B, which we simply formulate as $\text{Ru}_3(\text{CO})_{10}(\mu\text{-CO})$. Following a suggestion made by one of the reviewers, who questioned a structure with two coordinatively unsaturated metal centers, we propose a metal–metal double bond between the two CO-bridged metal atoms (cf. Scheme 3) in order to satisfy the 18-electron rule. Such a $\text{Ru}=\text{Ru}(\mu\text{-CO})$ unit was found, for example, in the case of the dinuclear complex $\text{Ru}_2(\mu\text{-CO})(\mu\text{-C}_2\text{Ph}_2)(\eta\text{-C}_5\text{H}_5)_2$.²⁹ Based on results obtained with ¹³C-labeled material (which “while not conclusive, ... suggest vibrational coupling of multiple bridging CO oscillators”) and some other observations, Bentsen and Wrighton¹⁰ favor a different structure with two bridging CO groups, $\text{Ru}_3(\text{CO})_9(\mu\text{-CO})_2$, where coordinative unsaturation is delocalized over two Ru–Ru bonds. Nevertheless, these authors also state that “the structure of CO-bridged $\text{M}_3(\text{CO})_{11}$ (M = Ru, Fe) cannot be determined with certainty from the available IR data”.

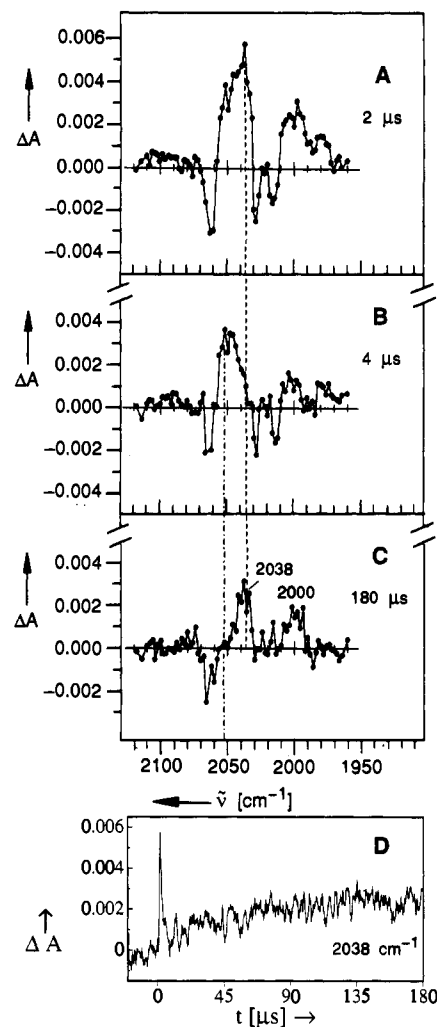


Figure 2. Flash photolysis (308 nm) of $\text{Ru}_3(\text{CO})_{12}$ (1, 0.6 mM) in cyclohexane under a 2:1 Ar–CO atmosphere at ambient temperature. (A) Transient CO stretching vibrational IR difference spectrum recorded after 2 μs . (B) Spectrum recorded after 4 μs . (C) Spectrum recorded after 180 μs . (D) Initial appearance and rapid decay of the photogenerated $\text{Ru}_3(\text{CO})_{10}(\mu\text{-CO})$ fragment (9-B) monitored at 2038 cm^{-1} , followed by the gradual grow-in of permanent product absorption.

photogenerated $\text{Ru}_3(\text{CO})_{10}(\mu\text{-CO})$ fragment (9-B) has already reacted with CO to re-form $\text{Ru}_3(\text{CO})_{12}$ during the 1–2- μs response time, such that only the very tail end of its decay is detected and accurate kinetic data cannot be evaluated.

However, much to our surprise, the accelerated trapping of 9-B by the added CO is not accompanied by more complete regeneration of the parent $\text{Ru}_3(\text{CO})_{12}$, in contrast to what might be expected from extrapolating the previously reported findings.¹¹ A significant amount of a hitherto unobserved species X, with a prominent absorption near 2050 cm^{-1} , is left behind when the very short-lived fragment 9-B has disappeared. This is evident from the transient IR difference spectrum displayed in Figure 2B, which illustrates the situation 4 μs after the flash excitation of $\text{Ru}_3(\text{CO})_{12}$ under 2:1 Ar–CO atmosphere. Subsequently occurring further spectral changes ultimately lead to a ν_{CO} pattern with prominent features around 2038 and 2000 cm^{-1} (Figure 2C). The gradual appearance of the band at 2038 cm^{-1} is best illustrated in Figure 2D, which covers a period of 180 μs . At this monitoring wavenumber, the intermediate species X is almost transparent (Figure 2B). However, its concurrent disappearance is clearly recognizable at 2056–2050 cm^{-1} , where the positive transient absorption returns to the base line. These observations indicate that the photogenerated $\text{Ru}_3(\text{CO})_{10}(\mu\text{-CO})$ fragment (9-B) reacts with CO not only to re-form the parent $\text{Ru}_3(\text{CO})_{12}$ but also to ultimately form products persisting on the time scale

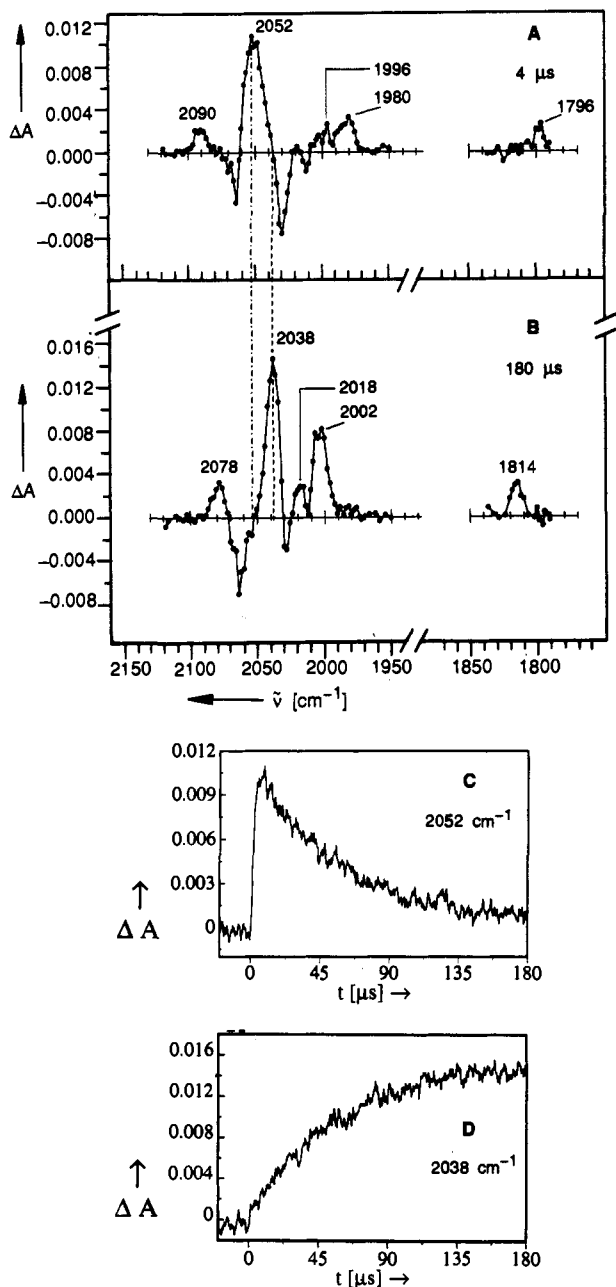


Figure 3. Flash photolysis (308 nm) of $\text{Ru}_3(\text{CO})_{12}$ (1, 0.6 mM) in cyclohexane under neat CO atmosphere at ambient temperature. (A) Transient CO stretching vibrational IR difference spectrum recorded after 4 μs . (B) Spectrum recorded after 180 μs . (C) Decay of the species assigned as $\text{Ru}_3(\text{CO})_{12}(\mu\text{-CO})$ (3) monitored at 2052 cm^{-1} . (D) Concurrent formation of the 1:1 mixture of $\text{Ru}_2(\text{CO})_9$ (5) and $\text{Ru}(\text{CO})_5$ (7) monitored at 2038 cm^{-1} .

of these experiments. This second process competes effectively at higher CO concentration and results in permanent consumption of $\text{Ru}_3(\text{CO})_{12}$.

These trends are magnified and clarified when the 308-nm flash photolysis of $\text{Ru}_3(\text{CO})_{12}$ is performed under an atmosphere of neat carbon monoxide. Under these conditions, the initially photogenerated $\text{Ru}_3(\text{CO})_{10}(\mu\text{-CO})$ fragment (9-B) is too short-lived for detection and is no longer observable. Instead, the spectral features associated with the aforementioned new intermediate species X appear almost instantaneously (Figure 3A). Moreover, comparing the band intensities with those in Figure 2B, we note an enhancement under CO atmosphere by a factor of ca. 3, which nicely parallels the increase in CO concentration. This applies also to the subsequently occurring spectral changes (Figure 3B) and thus confirms the above statement concerning

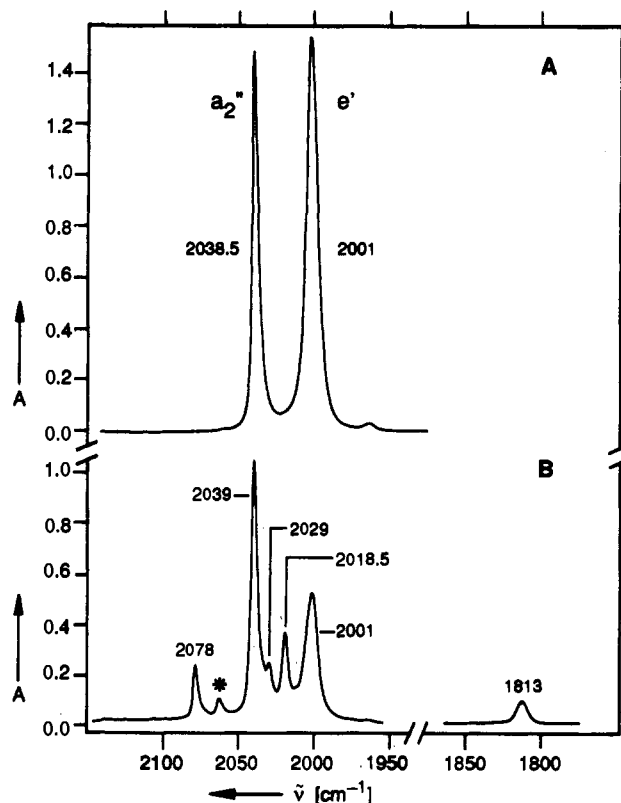


Figure 4. (A) CO stretching vibrational bands of $\text{Ru}(\text{CO})_5$ (7), generated in CO-saturated 2-methylpentane solution by irradiation ($\lambda \geq 370$ nm) of $\text{Ru}_3(\text{CO})_{12}$ (1). (B) Spectrum recorded after 60 min of continuous photolysis ($\lambda = 313$ nm) of the above solution of $\text{Ru}(\text{CO})_5$ (7) at -50°C , showing two-thirds conversion of 7 into $\text{Ru}_2(\text{CO})_9$ (5); the asterisk at 2062 cm^{-1} refers to the formation of a trace amount of 1.

the promotion of the route to the permanent product(s) via the intermediate species X in the presence of added CO in high concentration. Owing to this enhancement, weak product bands are rendered clearly observable in Figure 3, including those in the bridging CO region, which in the experiment under the 2:1 Ar-CO atmosphere (Figure 2) were below the detection level.

Apart from the $\text{Ru}_3(\text{CO})_{12}$ depletion bands, the final product spectrum (Figure 3B) shows four maxima at 2078 (m), 2038 (vst), 2018 (m), and 2002 (st) cm^{-1} in the terminal ν_{CO} region and one bridging CO band at 1814 (m) cm^{-1} . This latter feature, together with the terminal ν_{CO} bands at 2078 and 2018 cm^{-1} , is reminiscent of the frequency data reported for $\text{Ru}_2(\text{CO})_9$ (2077, 2018, and 1814 cm^{-1} in *n*-heptane),¹⁶ which were assigned⁴ to a structure similar to $\text{Os}_2(\text{CO})_9$, with one single CO bridge. The band positions at 2038 and 2002 cm^{-1} are in accord with the data reported for $\text{Ru}(\text{CO})_5$ [2035 (st) and 1999 (vst) cm^{-1}];¹⁷ 2038.9 (a_2'') and 2001.6 (e') cm^{-1} ,⁴ although the a_2'' vibration is too high in intensity, compared with the spectrum of pure $\text{Ru}(\text{CO})_5$ (Figure 4A). Hence it seems that at this position an additional strong absorption of $\text{Ru}_2(\text{CO})_9$ coincides with the a_2'' vibration of $\text{Ru}(\text{CO})_5$. A similar spectrum was reported by Bentsen and Wrighton¹⁰ from experiments involving long-wavelength photolysis of $\text{Ru}_3(\text{CO})_{12}$ in CO-saturated low-temperature solution.

In search of further, independent support for the assignment of the $\text{Ru}_2(\text{CO})_9$ bands in the above spectrum (Figure 3B), the photochemical generation of $\text{Ru}_2(\text{CO})_9$ (5) from $\text{Ru}(\text{CO})_5$ (7) (eq 1)^{4,16} was reexamined and monitored by means of conventional IR spectroscopy at low temperature. Previous spectroscopic studies were severely disturbed by the lability of the dinuclear complex at ambient temperature and by the concomitant

(16) Moss, J. R.; Graham, W. A. G. *J. Chem. Soc., Dalton Trans.* 1977, 95-99.

(17) Calderazzo, F.; L'Eplattenier, F. *Inorg. Chem.* 1967, 6, 1220-1224.

minima at 2064, 2030, and 2012 cm^{-1}) with a conventional IR spectrum of this complex (Table 1) reveals that the depletion band at 2064 cm^{-1} is somewhat reduced in intensity, thus indicating a partial overlap with the positive absorption of **3** at this position.

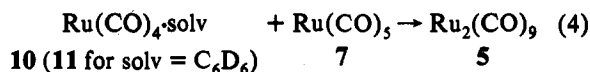
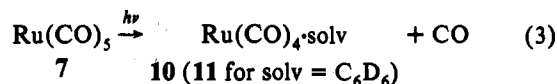
The spectral changes associated with the last process in Scheme 3, i.e., the conversion of $\text{Ru}_3(\text{CO})_{12}(\mu\text{-CO})$ (**3**) (Figure 3A) into the 1:1 mixture of $\text{Ru}_2(\text{CO})_9$ (**5**) and $\text{Ru}(\text{CO})_5$ (**7**) (Figure 3B), follow first-order kinetics, with $k = (2.2 \pm 0.4) \times 10^4 \text{ s}^{-1}$ throughout the entire spectral range. Both the decay of **3** (monitored at 2052 cm^{-1}) and the formation of **5** and **7** (monitored at 2038 cm^{-1}) are exemplarily displayed in Figures 3C and 3D. Unfortunately, it is difficult to assess whether or not the observed first-order rate constant is proportional to the CO concentration. At lower concentration of CO (i.e., under 2:1 Ar-CO atmosphere), the production of **3** and its subsequent conversion into **5** and **7** are accordingly reduced. This implies a rather poor signal-to-noise ratio (cf. Figure 2D), such that reliable kinetic data cannot be extracted. However, from a comparison of Figures 2D and 3D (or other pairs of transient signal traces at suitable monitoring wavenumbers), one gains the impression that in both experiments (i.e., under neat CO and 2:1 Ar-CO atmosphere) the spectral changes are terminated at nearly the same time (ca. 150–180 μs). While not conclusive, this observation suggests that the rate-determining step involves some spontaneous rearrangement of **3** rather than direct attack by carbon monoxide.

The dinuclear complex $\text{Ru}_2(\text{CO})_9$ (**5**) appears as a permanent product on the time scale (up to 100 ms) of these experiments with time-resolved IR detection at ambient temperature. Further reaction with CO to yield $\text{Ru}(\text{CO})_5$ (**7**) as the ultimate product^{3,4} is likely to occur in less than a few minutes, since monitoring the continuous irradiation of $\text{Ru}_3(\text{CO})_{12}$ (**1**) under CO atmosphere by means of conventional IR spectroscopy shows nothing but the gradual appearance of the pentacarbonyl complex. Accordingly, warming a cold solution of photogenerated $\text{Ru}_2(\text{CO})_9$ to ambient temperature was reported¹⁰ to result in the formation of $\text{Ru}(\text{CO})_5$.

B. Flash Photolysis of $\text{Ru}(\text{CO})_5$. The clean photochemical conversion of $\text{Ru}(\text{CO})_5$ (**7**) into $\text{Ru}_2(\text{CO})_9$ (**5**) in CO-containing solution (eq 1, Figure 4B) contrasts with the concurrent formation of a substantial amount of $\text{Ru}_3(\text{CO})_{12}$ (**1**) when, prior to the continuous irradiation at -50°C , the solution of $\text{Ru}(\text{CO})_5$ is thoroughly degassed and freed from dissolved carbon monoxide. This latter observation confirms previous results published by Moss and Graham.¹⁶ It aroused our curiosity about the mechanistic features of this process, the more so since $\text{Ru}(\text{CO})_5$ and $\text{Ru}_3(\text{CO})_{12}$ reportedly exist in a thermal equilibrium,²⁰ which is determined by the concentration of CO and in principle can be approached from either side. The proposed mechanism²⁰ of this thermal process involves reversible CO dissociation from $\text{Ru}(\text{CO})_5$ in the rate-determining step, followed by rapid reaction of the $\text{Ru}(\text{CO})_4$ fragment with $\text{Ru}(\text{CO})_5$ to generate $\text{Ru}_2(\text{CO})_9$ as an intermediate, which then, in an equally rapid second step, should add one more $\text{Ru}(\text{CO})_5$, to yield $\text{Ru}_3(\text{CO})_{12}$ with concurrent loss of two CO groups. Flash photolysis of $\text{Ru}(\text{CO})_5$

in the gas phase²¹ is known to yield the two fragments $\text{Ru}(\text{CO})_4$ and $\text{Ru}(\text{CO})_3$, which were shown, by means of time-resolved IR spectroscopy, to either recombine with CO or react with parent $\text{Ru}(\text{CO})_5$, forming dinuclear products. However, information on the transient existence and reactivity of such fragments in solution is marginal. We are now in a position to communicate some pertinent preliminary results.

In solution at ambient temperature, $\text{Ru}(\text{CO})_5$ (**7**) is only moderately stable and decomposes slowly in the absence of added CO. Therefore, the reservoir with a CO-free stock solution of $\text{Ru}(\text{CO})_5$ in methylcyclohexane (used instead of cyclohexane, mp 6.5 $^\circ\text{C}$) was kept at -20°C , and the flash photolysis experiments were performed in an infrared cell cooled to $5 \pm 2^\circ\text{C}$. Exploratory experiments under argon atmosphere indicate the photolytic generation of a rather short-lived species observable at monitoring wavenumbers ranging from 1990 to 1940 cm^{-1} . It decays within a period of less than 4–5 μs with concurrent formation of $\text{Ru}_2(\text{CO})_9$ (**5**), which is identified on the basis of product absorptions growing in at 2078, \sim 2022 and 1814 cm^{-1} (cf. Table 1). Based on this observation, and by comparison with the CO stretching vibrational pattern of $\text{Fe}(\text{CO})_4\text{solv}$,²² the short-lived transient is assigned as $\text{Ru}(\text{CO})_4\text{solv}$ (**10**) (eqs 3 and 4), although the spectral resolution was poor and a weak high-frequency band expected around 2080–2100 cm^{-1} could not be detected.



By analogy with the relatively long-lived $\text{M}(\text{CO})_4\text{-C}_6\text{D}_6$ species of iron²³ and osmium,²⁴ the $\text{Ru}(\text{CO})_4$ fragment is trapped in the form of its C_6D_6 adduct (**11**, solv = C_6D_6) when the flash photolysis of $\text{Ru}(\text{CO})_5$ (eq 3) is performed in the presence of benzene- d_6 .²⁵ The transient CO stretching vibrational difference spectrum displayed in Figure 6A is observed upon 308-nm flash photolysis of $\text{Ru}(\text{CO})_5$ (**7**) under argon atmosphere in methylcyclohexane doped with ca. 10% benzene- d_6 .²⁶ In addition to the depletion bands of the starting material, with minima at 2038 and 2000 cm^{-1} (cf. Figure 4A and Table 1), this spectrum shows four positive absorptions, three of which [2096 (w), 1984 (st), and 1958 (st) cm^{-1}] exhibit analogous kinetic behavior and therefore are attributed to the selfsame species, $\text{Ru}(\text{CO})_4\text{-C}_6\text{D}_6$ (**11**). The assignment of the remaining weak band near 2070 cm^{-1} is less straightforward.²⁷ The ν_{CO} intensity pattern of **11** compares well with that of the analogous iron compound, $\text{Fe}(\text{CO})_4\text{-C}_6\text{D}_6$,²³ which is thought to possess C_{2v} symmetry. The high-frequency weak band and the two strong bands at lower frequencies in the spectrum of **11** are therefore assigned to the a_1 , b_1 , and b_2 CO stretching vibrations. The missing second a_1 band should be of low to

(21) Bogdan, P. L.; Weitz, E. *J. Am. Chem. Soc.* **1989**, *111*, 3163–3167.

(22) Grevels, F.-W. In *Photoprocesses in Transition Metal Complexes, Biosystems and other Molecules. Experiment and Theory*; Kochanski, E., Ed.; NATO ASI Series C 376; Kluwer Academic Publishers: Dordrecht, 1992; pp 141–171.

(23) Church, S. P.; Grevels, F.-W.; Hermann, H.; Kelly, J. M.; Klotzbücher, W. E.; Schaffner, K. *J. Chem. Soc., Chem. Commun.* **1985**, 594–596.

(24) Church, S. P.; Grevels, F.-W.; Kiel, G.-Y.; Kiel, W. A.; Takats, J.; Schaffner, K. *Angew. Chem.* **1986**, *98*, 993–994; *Angew. Chem., Int. Ed. Engl.* **1986**, *25*, 991–992.

(25) In the relevant IR spectral region slightly below 2000 cm^{-1} , C_6H_6 shows a relatively strong absorption, which is absent in the case of the deuterated solvent C_6D_6 .

(26) The influence of varying concentrations of benzene- d_6 , $\text{Ru}(\text{CO})_5$ (**7**), and CO on the decay of $\text{Ru}(\text{CO})_4\text{(solv/C}_6\text{D}_6)$ (**10**, **11**) and on the competitive formation of $\text{Ru}_2(\text{CO})_9$ (**5**) and re-formation of **7** is a matter of current investigations, which place emphasis on the quantitative aspects of a comprehensive kinetic scheme. This is beyond the scope of the present paper, which primarily aims at the spectroscopic characterization of the involved species.

(19) As an alternative route to the photodissociative pathway (**1** \rightarrow **9-T** \rightarrow **9-B** \rightarrow **1-B** \rightarrow **3**), the formation of the $\text{Ru}_3(\text{CO})_{12}(\mu\text{-CO})$ species **3** could also take place via direct photoisomerization of the parent $\text{Ru}_3(\text{CO})_{12}$ (**1** \rightarrow **1-B** \rightarrow **3**; cf. Scheme 1). This could occur if the dissociative excited state of $\text{Ru}_3(\text{CO})_{12}$, populated by short-wavelength excitation, to some extent decays by internal conversion to the low-energy excited state, which has been proposed to undergo structural rearrangement to form the CO-bridged isomer **1-B**.^{1,6,9} Unfortunately, our experiments do not provide clear-cut information in this respect, neither in favor of nor against the latter route. Under 2:1 Ar-CO atmosphere (Figure 2), where the two species **9-B** and **3** are observable in the selfsame experiment, all signals are unfavorably weak, and both the decay of **9-B** (cf. the narrow spike in Figure 2D) and the rise of absorptions associated with **3** are terminated in less than 4 μs . Therefore, the coincidence of these spectral changes, which would be indicative of the photodissociative route, is difficult to assess. Hence we cannot state with certainty whether or not the dissociative mechanism operates exclusively in the overall process.

(20) Hastings, W. R.; Roussel, M. R.; Baird, M. C. *J. Chem. Soc., Dalton Trans.* **1990**, 203–205.

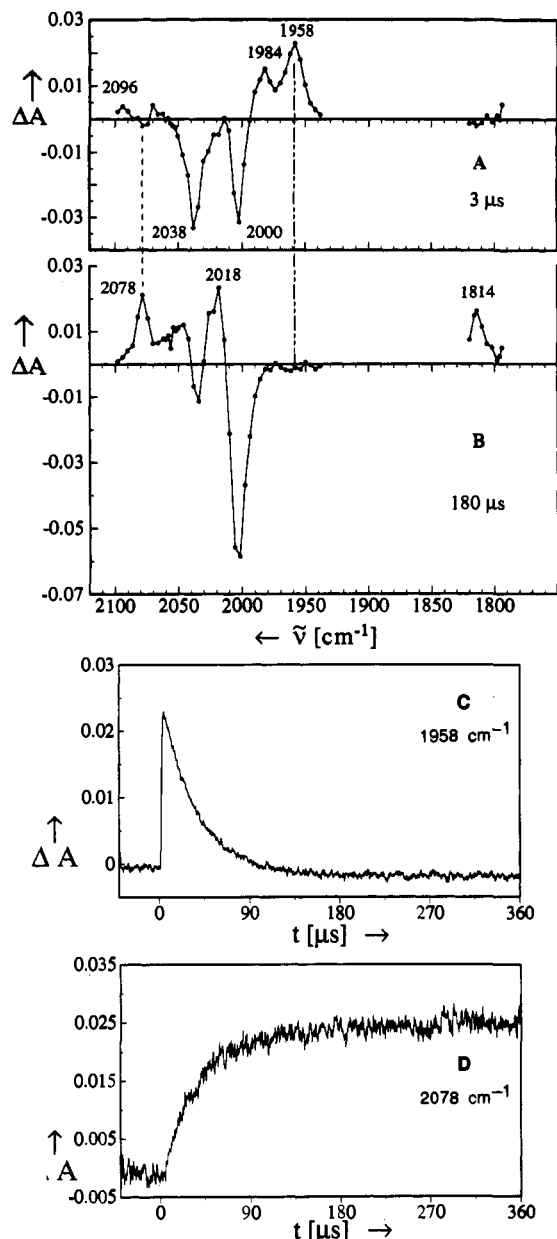


Figure 6. Flash photolysis (308 nm) of $\text{Ru}(\text{CO})_5$ (7, 0.9 mM) in methylcyclohexane, doped with ca. 10% benzene- d_6 , under Ar atmosphere at 5 °C. (A) Transient CO stretching vibrational IR difference spectrum recorded after 3 μs . (B) Spectrum recorded after 180 μs . (C) Decay of $\text{Ru}(\text{CO})_4\text{C}_6\text{D}_6$ (11) monitored at 1958 cm^{-1} . (D) Concurrent formation of $\text{Ru}_2(\text{CO})_9$ (5) monitored at 2078 cm^{-1} .

moderate intensity with a position in the lower frequency region; it could thus either be canceled out due to overlap with the e' depletion band of the parent $\text{Ru}(\text{CO})_5$ (7) (which in fact shows a slightly reduced intensity) or be buried underneath the strong b_1/b_2 absorptions.

The decay of $\text{Ru}(\text{CO})_4\text{C}_6\text{D}_6$ (11) results in the formation of $\text{Ru}_2(\text{CO})_9$ (5) (eq 4), as indicated by the characteristic bands growing in at 2078, 2018, and 1814 cm^{-1} (Figure 6B, cf. Table 1). The spectral changes follow approximate first-order kinetics [$k = (3 \pm 0.3) \times 10^4 \text{ s}^{-1}$] and are terminated after 90–100 μs ,

(27) Careful comparative examination of Figures 6A and 7A reveals that the very weak negative feature at 2078 cm^{-1} in Figure 6A possibly represents the photodepletion of a trace amount of $\text{Ru}_2(\text{CO})_9$ (5). This would imply that a small proportion (on the order of 5–10%) of the irradiated sample solution was left behind in the IR cell when, between two laser shots, the system was emptied and refilled with fresh stock solution. If so, the unidentified positive feature near 2070 cm^{-1} in Figure 6A could be attributed to the resulting photoproduct of 5, presumably $\text{Ru}_2(\text{CO})_8$ (12).

as it is exemplarily illustrated in Figure 6C (decay of 11) and Figure 6D (formation of 5). The postphotolytic consumption of $\text{Ru}(\text{CO})_5$ (7) according to eq 4 is clearly recognizable on the basis of the respective further depletion of its e' band around 2000 cm^{-1} (compare Figures 6A and 6B). This in turn indicates that the possible competitive re-formation of the starting material 7 by reaction of 11 with photodissociated CO is, at best, of minor importance under the conditions employed in this experiment.²⁶ The concomitant decrease in intensity of the a_2'' $\text{Ru}(\text{CO})_5$ depletion band at 2038 cm^{-1} is due to the overlap with the strongest ν_{CO} absorption of the product, $\text{Ru}_2(\text{CO})_9$ (5) (cf. Figures 4 and 5 and Table 1), the onset of which is recognizable in Figure 6B near 2050 cm^{-1} .

In the context of the conversion of $\text{Ru}(\text{CO})_5$ (7) into $\text{Ru}_3(\text{CO})_{12}$ (1), it is important to note that the dinuclear $\text{Ru}_2(\text{CO})_9$ complex (5) is stable on the time scale of this experiment (cf. Figure 6D), with no indication of $\text{Ru}_3(\text{CO})_{12}$ formation. Even when the absorption of $\text{Ru}_2(\text{CO})_9$ at 2078 cm^{-1} is monitored over an extended period (up to 1 s), a decrease is barely recognizable and does not exceed 5–10%. Hence, it is evident that the thermal reaction of $\text{Ru}_2(\text{CO})_9$ with $\text{Ru}(\text{CO})_5$, proposed to yield $\text{Ru}_3(\text{CO})_{12}$ with concurrent loss of two CO,²⁰ is slower by at least 5–6 orders of magnitude when compared with the formation of the dinuclear complex in the preceding step (eq 4). However, this is not very surprising in view of the fact that both $\text{Ru}_2(\text{CO})_9$ (5) and $\text{Ru}(\text{CO})_5$ (7) are coordinatively saturated compounds, whereas the $\text{Ru}(\text{CO})_4$ solv fragment affords a vacant coordination site readily accessible (even in the case of 11, with solv = C_6D_6) to the $\text{Ru}(\text{CO})_5$ reactant, such that the formation of $\text{Ru}_2(\text{CO})_9$ is fast.

Based on this finding, we suspect that the photochemical formation of $\text{Ru}_3(\text{CO})_{12}$ (1), observed upon continuous irradiation of $\text{Ru}(\text{CO})_5$ (7) at –50 °C in degassed CO-free solution (*vide supra*, cf. ref 16), involves photolytic CO dissociation not only from the starting material but also from the *in situ* generated $\text{Ru}_2(\text{CO})_9$ (5). Unfortunately, the latter compound is too unstable and too difficult to handle (as to generate and store a stock solution containing this complex) to be useful in a flash photolytic study.

As a makeshift approach, some flash photolysis experiments with a degassed stock solution of $\text{Ru}(\text{CO})_5$ (7) under argon atmosphere were performed in such a way that only a part (ca. 30–40%) instead of the whole content of the IR sample cell was replaced by fresh stock solution during the interval of several seconds between the laser shots. In this way, a mixture of $\text{Ru}(\text{CO})_5$ (7) and *in situ* generated $\text{Ru}_2(\text{CO})_9$ (5) (with nearly stationary concentrations) was photolyzed in each individual shot. This is documented by the transient difference spectrum recorded 2.5 μs after flash excitation (Figure 7A). It shows a depletion band pattern, which compares well with the positive band patterns displayed in Figures 3B and 4B and thus reveals that, in addition to $\text{Ru}(\text{CO})_5$ (7, minima at 2036 and 2002 cm^{-1}), a substantial amount of $\text{Ru}_2(\text{CO})_9$ (5, minima at 2078, 2036, 2018, and 1814 cm^{-1}) has disappeared upon flash photolysis of the sample solution. The generation of $\text{Ru}(\text{CO})_4\text{C}_6\text{D}_6$ (11) from $\text{Ru}(\text{CO})_5$ again is readily recognized on the basis of the positive product absorptions at 2094, 1986, and 1958 cm^{-1} in Figure 7A (cf. Table 1). What remains to be discussed is the product arising from the photolysis of $\text{Ru}_2(\text{CO})_9$ (5), the $\text{Ru}_2(\text{CO})_8$ fragment (12) being the logical candidate. The analogous osmium species, $\text{Os}_2(\text{CO})_8$,²⁸ exhibits three prominent ν_{CO} bands at 2058, 2018, and 2003 cm^{-1} (in

(28) (a) Grevels, F.-W.; Klotzbücher, W. E.; Seils, F.; Schaffner, K.; Takats, J. J. *Am. Chem. Soc.* **1990**, *112*, 1995–1996. (b) Haynes, A.; Poliakoff, M.; Turner, J. J.; Bender, B. R.; Norton, J. R. *J. Organomet. Chem.* **1990**, *383*, 497–519.

(29) Colborn, R. E.; Dyke, A. F.; Gracey, B. P.; Knox, S. A. R.; Macpherson, K. A.; Mead, K. A.; Orpen, A. G. *J. Chem. Soc., Dalton Trans.* **1990**, 761–771.

(30) (a) Adams, R. D.; Chi, Y.; DesMarteau, D. D.; Lentz, D.; Marschall, R. J. *Am. Chem. Soc.* **1992**, *114*, 1909–1910. (b) Adams, R. D.; Chi, Y.; DesMarteau, D. D.; Lentz, D.; Marschall, R.; Scherrmann, A. *J. Am. Chem. Soc.* **1992**, *114*, 10822–10826.

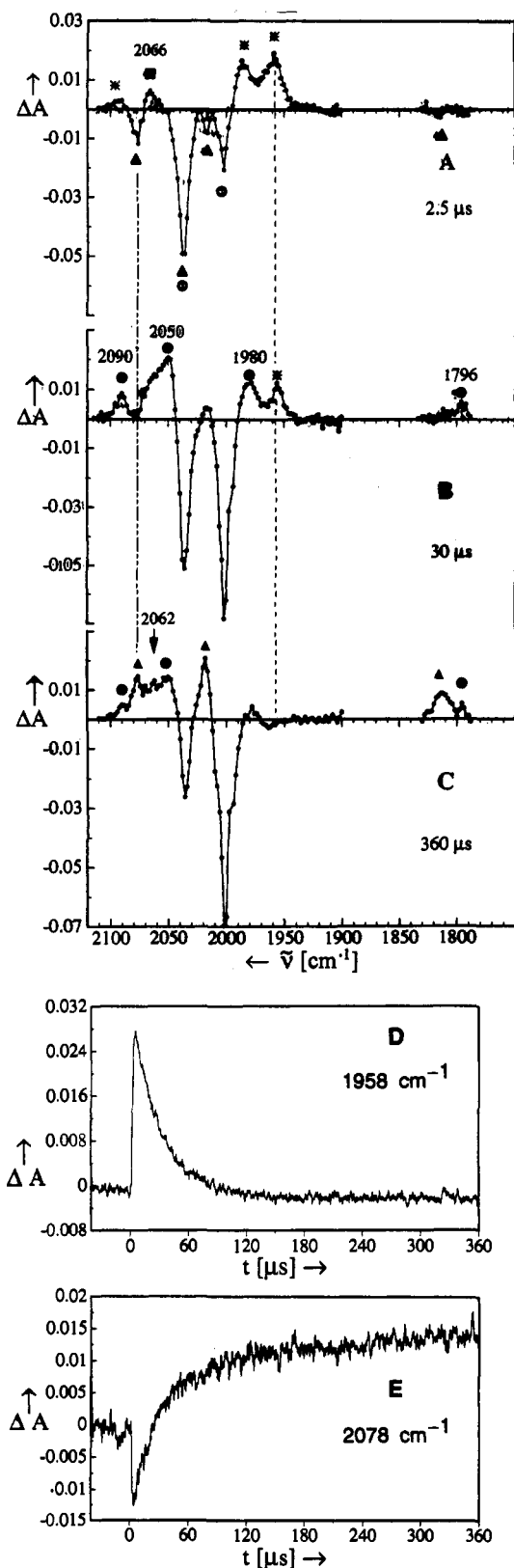
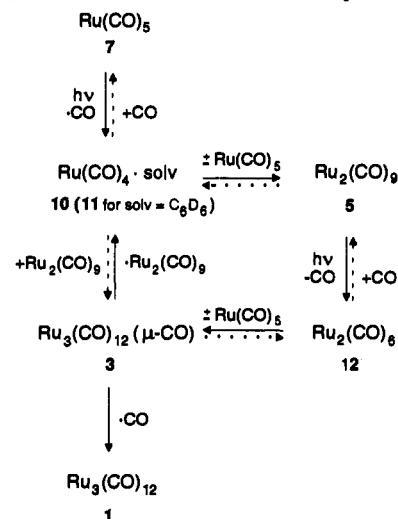


Figure 7. Flash photolysis (308 nm) of $\text{Ru}(\text{CO})_5$ (7, 0.8 mM) and *in situ* generated $\text{Ru}_2(\text{CO})_9$ (5, see text) in methylcyclohexane, doped with ca. 10% benzene- d_6 , under Ar atmosphere at 5 °C. (A) Transient CO stretching vibrational IR difference spectrum recorded after 2.5 μs . (B) Spectrum recorded after 30 μs . (C) Spectrum recorded after 360 μs . (D) Decay of $\text{Ru}(\text{CO})_4\cdot\text{C}_6\text{D}_6$ (11) monitored at 1958 cm^{-1} . (E) Initial photodepletion and subsequent grow-in of $\text{Ru}_2(\text{CO})_9$ (5) monitored at 2078 cm^{-1} . The symbols represent the following species: (*) $\text{Ru}(\text{CO})_4\cdot\text{C}_6\text{D}_6$ (11); (■) $\text{Ru}_2(\text{CO})_8$ (12); (○) $\text{Ru}(\text{CO})_5$ (7); (▲) $\text{Ru}_2(\text{CO})_9$ (5); (●) $\text{Ru}_3(\text{CO})_{12}(\mu\text{-CO})$ (3); (↓) $\text{Ru}_3(\text{CO})_{12}$ (1).

Scheme 4. Reactions Occurring upon Flash Photolysis (308 nm) of $\text{Ru}(\text{CO})_5$ (7) or a Mixture of 7 and *in Situ* Photogenerated $\text{Ru}_2(\text{CO})_9$ (5) in Hydrocarbon Solution as Monitored by Means of Time-Resolved IR Spectroscopy



cyclohexane). Thus, allowing for moderate frequency shifts in going from osmium to ruthenium, it seems reasonable to assign the positive absorption at 2066 cm^{-1} in Figure 7A as the high-frequency CO stretching vibration of 12. The other two expected bands of this species could be canceled by overlap with the depletion bands of 5 and 7 in the region from 2000 to 2020 cm^{-1} and thus remain obscured.

Subsequently occurring processes give rise to spectral changes, which are interwoven in the frequency and time domains. First of all, the solvated $\text{Ru}(\text{CO})_4$ species 11 (solv = C_6D_6) expectedly decays with concurrent formation of $\text{Ru}_2(\text{CO})_9$ (5) (eq 4). This reaction essentially follows the same kinetics as observed in the previous experiment (cf. Figure 6). It is terminated after ca. 90 μs , as can be seen from Figure 7D, which shows the decay of $\text{Ru}(\text{CO})_4\cdot\text{C}_6\text{D}_6$ (11) monitored at 1958 cm^{-1} . During this period, the absorbance of $\text{Ru}_2(\text{CO})_9$ (5) at 2078 cm^{-1} (Figure 7E) grows in from negative to positive ΔA values. The spectrum displayed in Figure 7B illustrates the situation at an intermediate time (30 μs), when the absorbance of 5 in Figure 7E passes through the initial base-line level, such that all bands associated with this complex are absent in the transient difference spectrum. At this stage, some of species 11 is still present, but the spectrum is dominated by several new features. We note maxima at 2090, 2050, 1980, and 1796 cm^{-1} , which are reminiscent of the ν_{CO} pattern associated with $\text{Ru}_3(\text{CO})_{12}(\mu\text{-CO})$ (3) (cf. Figure 3A and Table 1). This species could originate either from the addition of $\text{Ru}(\text{CO})_5$ (7) to $\text{Ru}_2(\text{CO})_8$ (12) or from the reaction of the solvated $\text{Ru}(\text{CO})_4$ fragment 11 with $\text{Ru}_2(\text{CO})_9$ (5). However, the latter process should be of minor importance because these two reactants are present only in low concentration, compared with the large excess of unphotolyzed $\text{Ru}(\text{CO})_5$.

These findings and considerations are summarized in Scheme 4. Included is the ultimately occurring decay of $\text{Ru}_3(\text{CO})_{12}(\mu\text{-CO})$ (3), which is clearly observable in going from Figure 7B to Figure 7C. It involves two different reactions: loss of CO with formation of $\text{Ru}_3(\text{CO})_{12}$ (1) and breakdown of the trinuclear cluster core with re-formation of some $\text{Ru}_2(\text{CO})_9$ (5).

The latter process is recognized by comparative examination of Figures 7D and 7E, which reveals that the grow-in of the absorbance of $\text{Ru}_2(\text{CO})_9$ (5) at 2078 cm^{-1} is not terminated after 90 μs , when the signal at 1958 cm^{-1} of its immediate precursor $\text{Ru}(\text{CO})_4\cdot\text{C}_6\text{D}_6$ (11) has completely disappeared. Beyond this period, some additional $\text{Ru}_2(\text{CO})_9$ (5) is formed, concurrent with the further decay of 3. This reaction differs from the decay of

3 under CO atmosphere, illustrated in Figure 3, which yields $\text{Ru}_2(\text{CO})_9$ (**5**) and $\text{Ru}(\text{CO})_5$ (**7**) in a 1:1 ratio (Scheme 3).

Loss of CO from $\text{Ru}_3(\text{CO})_{12}(\mu\text{-CO})$ (**3**) provides a rationale for the formation of $\text{Ru}_3(\text{CO})_{12}$ (**1**) in large quantity upon low-temperature continuous irradiation of $\text{Ru}(\text{CO})_5$ (**7**) in CO-free solution, as monitored by means of conventional IR spectroscopy (*vide supra*, cf. ref 16). Unfortunately, the evidence for the formation of **1** in the present experiment with time-resolved IR detection is less striking, since the ultimate spectrum (Figure 7C), recorded 360 μs after the flash excitation, is dominated by the positive absorptions associated with $\text{Ru}_2(\text{CO})_9$ (**5**). Only a weak maximum is observed at 2062 cm^{-1} in Figure 7C, which is attributable to the strongest CO stretching vibration of $\text{Ru}_3(\text{CO})_{12}$ (**1**). Further irradiation would be necessary to convert a substantial amount of the dinuclear complex **5** into the trinuclear cluster **1**.

Under analogous photolytic conditions in the same saturated hydrocarbon solvent (methylcyclohexane), but in the absence of added benzene- d_6 , a transient difference spectrum quite similar to that displayed in Figure 7B is observed shortly (4 μs) after flash excitation of $\text{Ru}(\text{CO})_5$ (**7**) and *in situ* photogenerated $\text{Ru}_2(\text{CO})_9$ (**5**). It is dominated by the positive absorption pattern associated with $\text{Ru}_3(\text{CO})_{12}(\mu\text{-CO})$ (**3**) and by the depletion bands of **7**, whereas the initial photodepletion of **5** could not be detected in this case. This is due to the very fast trapping of the weakly solvated $\text{Ru}(\text{CO})_4\text{solv}$ (**10**) by $\text{Ru}(\text{CO})_5$ (**7**) to form $\text{Ru}_2(\text{CO})_9$ (**5**) (eq 4), which almost instantaneously compensates for the photolytic consumption of **5**. Again, the final spectrum (360 μs after flash excitation) is dominated by the positive ν_{CO} pattern of **5** and the depletion bands of **7**, with a small amount of $\text{Ru}_3(\text{CO})_{12}$ (**1**) being barely recognizable.

Exploratory experiments involving flash photolysis of $\text{Ru}(\text{CO})_5$ (**7**) under CO atmosphere²⁶ indicate that the production of $\text{Ru}_2(\text{CO})_9$ (**5**) is drastically reduced (by a factor on the order of 10), apparently as a result of competitive trapping of photogenerated $\text{Ru}(\text{CO})_4\text{solv}$ (**10**, **11**) by carbon monoxide, such that the starting material **7** is largely regenerated. This should also apply to the

fate of the $\text{Ru}_2(\text{CO})_8$ fragment (**12**), following its photolytic generation from *in situ* produced **5**. Altogether, this provides a rationale for the failure of the photolysis of **7** in the presence of dissolved CO to produce more than a trace amount of $\text{Ru}_3(\text{CO})_{12}$ (**1**) (cf. Figure 4).

Conclusion

This study has demonstrated that $\text{Ru}_3(\text{CO})_{12}$ (**1**) and $\text{Ru}(\text{CO})_5$ (**7**) are interconvertible upon short-wavelength irradiation (308 nm), whereby the concentration of dissolved carbon monoxide plays a crucial role. Following the initial photolytic generation of the fragments $\text{Ru}_3(\text{CO})_{11}$ (**9**) and $\text{Ru}(\text{CO})_4\text{solv}$ (**10**, **11**), respectively, the species $\text{Ru}_3(\text{CO})_{13}$ (**3**) and $\text{Ru}_2(\text{CO})_9$ (**5**) are observed as common intermediates in either direction (Schemes 3 and 4). Regarding the photolytic behavior of **1**, these findings underline that the breakdown of the trinuclear cluster framework does not necessarily require long-wavelength excitation, thus complementing previous investigations into the wavelength-dependent photochemistry of **1**.^{1,6,9} It seems that the ability of the photogenerated $\text{Ru}_3(\text{CO})_{11}$ fragment 9-T to form the CO-bridged isomer 9-B is essential for the observed reactivity of **1** in the presence of CO in high concentration.

The results of this flash photolytic investigation should analogously be applicable to the respective thermally induced reactions, thus providing deeper insight into the course of events. Considering the mechanistic implications of the conversion of $\text{Ru}(\text{CO})_5$ (**7**) into $\text{Ru}_3(\text{CO})_{12}$ (**1**), for example, we note that the intermediately formed $\text{Ru}_2(\text{CO})_9$ (**5**) is a relatively long-lived species. In consequence of this, reversible CO dissociation from both $\text{Ru}(\text{CO})_5$ (**7**) and $\text{Ru}_2(\text{CO})_9$ (**5**) should be equally relevant to the overall kinetics of the thermally induced process and thus should be explicitly accounted for in a thorough investigation.

Acknowledgment. We are indebted to Mr. K. Kerpen, Mrs. G. Klihm, and Miss D. Pagirius for skilled technical assistance. Helpful and constructive comments by the reviewers are gratefully acknowledged.